Fixed-Time Consensus for Multi-Agent Systems under Switching Topology based on A Distributed Zeroing Neural Network Method

Lin Xiao, Jiajie Luo, Jichun Li, Lei Jia, Jiguang Li

***Abstract*—The zeroing neural network (ZNN) has been uilized in various control applications such as tracking and motion control. While ZNN has been widely employed, its utilization in consensus control schemes is rarely reported. In this study, we propose a novel distributed fixed-time zeroing neural network (DFTZNN) scheme designed to achieve fixed-time and robust consensus in multi-agent systems operating under a switching topology. Theoretical analysis is provided to establish the fixed-time stability and robustness of the proposed scheme in the presence of bounded noises. To highlight the superiority of the proposed method, we introduce an example demonstrating the estimation of the upper bound of a settling-time function. Theoretical analysis and a novel upper bound estimation method are subsequently validated through numerical experiments, including a practical application in formation control. The comprehensive theoretical and simulation results demonstrate the superior performance of the DFTZNN scheme under both fixed and switching topologies, establishing it as a novel and systematic framework for designing consensus control schemes.**

***Index Terms*—Zeroing neural network, fixed-time consensus, switching topology, multi-agent systems.**

I. Introduction

Inspired by the observed phenomenon of biological swarming in nature, multi-agent system is a complex system first proposed by Minsky [1]. This system is comprised of a multitude of agents engaging in interactions, cooperation, and mutual influence. A multi-agent system has three characteristics: local communication, autonomy, and distributed control. In recent years, advancements in robotics, sensing technology, and communication technology have spurred rapid developments in the theory of complex dynamic networks. This area has emerged as a prominent research focus within the field of artificial intelligence. Researchers use complex dynamic networks to describe multi-agent systems, and it gradually plays a crucial role in a variety of applications, including drone formations [2], transportation systems [3], building automation [4], underwater exploration [5], and surveillance systems [6], etc.

Consensus is a fundamental challenge in coordinating multi-agent systems [7]–[9] encompassing diverse applications such as flocking [10], attitude alignment [11], and formation control [2], [10]. Consensus refers to the collaborative sharing of information among all agents within the system through a network, leading to the attainment of an agreement on key information over a period of time. The key in addressing the consensus problem is to design an appropriate consensus control protocol, ensuring that the states of all agents converge towards a consensus. Olfati-Saber and Murray [12] introduced a linear consensus protocol as a solution to the problem. Nonlinear protocols become relevant when there is observability of a nonlinear function in the agent state of interest or when achieving finite-time consensus is a specific requirement. In such cases, nonlinear approaches are considered for a more tailored and effective solution [13].

The convergence rate is important in the field of consensus. Based on distinct convergence rates, research in consensus can be categorized into asymptotically consensus control [14], finite-time consensus [13] and fixed-time consensus [15]. While a finite-time consensus system exhibits a definite convergence time, its effectiveness depends closely on the initial state of the multi-agent system. This characteristic introduces limitations in practical applications [16]. In contrast, the fixed-time consensus proves to be a more practical approach. This is because the initial design parameters rather than the initial states of multi-agent systems to determine the bound of settling-time function [17]. Researchers also develop various methods to estimate the upper bound of the settling time for a fixed-time convergent system, with Polyakov's theorem [18] being one of these established methods.

Many algorithms have been proposed in the field of consensus. However, most of them lack systematic and general applicability. It would be advantageous to employ a general framework for addressing the consensus problem. The zeroing neural network (ZNN), as a systematic tool, stands out as an ideal candidate for designing appropriate protocols in numerous control applications such as tracking [19] and motion control [20], etc. Based on existing systematic studies on ZNN, engineers can customize the desired control protocol easily. They have many choices to choose from since there are a variety of ZNNs with advanced features including finite-time convergence [21], complex-valued process [22], noise-tolerant model [23], etc.

This work was supported in part by the Natural Science Foundation of Hunan Province of China under Grant 2022RC1103 and Grant 2021JJ20005, and in part by the National Natural Science Foundation of China under Grant 61866013.

Lin Xiao and Lei Jia are with the Hunan Provincial Key Laboratory of Intelligent Computing and Language Information Processing and Ministry of Education Key Laboratory of Computing and Stochastic Mathematics (MOE-LCSM), Hunan Normal University, Changsha 410081, China (e-mail: xiaolin860728@163.com).

Jiajie Luo and Jichun Li are with the school of computing, Newcastle University, UK.

Jiguang Li is with the Hangzhou fortunelight technology Inc, Hangzhou 311200, China.

The multi-agent systems often operate in complex environments [10], [24], [25]. The communication networks among agents may not be stable [26], [27]. Various noises may also be present in the operational environment. For instance, the communication topology may be dynamic, involving switching scenarios [28], [29], and truncation errors can arise during the analog circuit implementation. In this study, we present a novel approach called the distributed fixed-time zeroing neural network (DFTZNN) scheme, designed to achieve both fixed-time and robust consensus in multi-agent systems. We conduct a thorough theoretical analysis to investigate the fixed-time and robust consensus under a switching topology using the DFTZNN. Additionally, we illustrate the superiority of the DFTZNN by estimating the upper bound of the settling-time function. This estimation is performed using a novel integral-based method [30]. Furthermore, we compare the results with the upper bound estimated using the traditional method based on Polyakov's theorem [18].

The rest of this paper is organized as follows. In Section II, we provide an overview of the basic concepts and related theories. In Section III, we introduce the design process of the practical consensus scheme and the concept of fixed-time convergence. In Section IV describes a detailed theoretical analysis of the proposed scheme, including the estimation of the upper bound using both the traditional method based on Polyakov's theorem and a novel integral-based method. In Section V presents numerical experiments conducted under both fixed and switching topologies to validate the fixed-time and robust consensus. Additionally, we demonstrate the application of fixed-time and robust consensus in formation control. Moreover, as the most popular application in multi-agent systems, the fixed-time and robust consensus in formation control is shown. Finally, Section VI discusses the conclusions drawn from this study. The main contributions of this study are listed below:

1) We introduce a new perspective for designing suitable control schemes in multi-gent system. Based on the ZNN approach, the DFTZNN scheme is proposed for achieving both fixed-time and robust consensus.
2) We provide a comprehensive theoretical analysis to establish the fixed-time stability and robustness of the proposed scheme. The analysis also includes the presentation of the upper bound of the error in the presence of bounded noise.
3) Building upon the theoretical foundation of a novel integral-based method, we estimate the upper bound of the settling-time function. For comparison, we also present the traditional upper bound estimation method and highlight the superior performance of the proposed integral-based approach.
4) We analyze and validate the fixed-time consensus of the DFTZNN scheme under a switching topology, a more realistic scenario in real-life applications compared to a fixed topology. Furthermore, we successfully apply the DFTZNN scheme to achieve formation control.

II. Preliminaries

A. The Graph Theory

In this paper, a communication topology consisting of n vertices can be represented as a graph:

$$G = (V, E), \tag{1}$$

where $V = \{v_1, v_2, v_3...v_n\}$ denotes a finite set of vertices (or nodes), and $E \subseteq V \times V$ represents the relationship between two nodes, called edges. Such a graph is called a strongly connected graph if and only if there exists a communication path between any two nodes.

The adjacency matrix A of graph G with n vertices is a square matrix that indicates whether pairs of vertices are adjacent or not in the graph. It can be denoted as $A = [a_{ij}]$ with a_{ij} being:

$$a_{ij} = \begin{cases} 1, & \text{if } j \in N_i, \\ 0, & \text{otherwise}, \end{cases} \tag{2}$$

where N_i represents a set of the adjacent nodes of v_i.

The in-degree and out-degree of node v_i are defined as follows:

$$\deg_{\text{in}}(v_i) = \sum_{j=1}^{n} a_{ji}, \quad \deg_{\text{out}}(v_i) = \sum_{j=1}^{n} a_{ij}. \tag{3}$$

The degree matrix D is a diagonal matrix in the form $\text{diag}\{d_1, d_2, d_3...d_n\}$ where d_i is represented as follows:

$$d_i = \deg_{\text{out}}(v_i) = \sum_{j=1}^{n} a_{ij}. \tag{4}$$

Using the adjacency matrix and degree matrix, a Laplacian matrix can be represented as

$$L = D - A. \tag{5}$$

Lemma 1 *([12]) Suppose that graph G denotes a strongly connected graph, L denotes the Laplacian matrix of graph G, and $\boldsymbol{x}$ denotes the state vector of the multi-agent system with a communication topology G, then $L\boldsymbol{x} = 0$ if and only if $\boldsymbol{x} \in \mathbb{I}^n = \left\{ \boldsymbol{y} \in \mathbb{R}^n | \boldsymbol{y} = c \cdot (1, 1, 1....1)^T \right\}$.*

B. Switching Topology

Let's consider a dynamic system consisting of n mobile agents, all with the common objective of reaching an agreement on a specific interest. Indeed, the communication topology within a system may switch over time. Neglecting this dynamic aspect in the consensus protocol could result in control failures. Therefore, it is imperative to discuss and account for the possibility of switching topology to ensure the robustness and effectiveness of the consensus protocol.

For the subsequent discussion, let $\mathcal{Q}$ be the set denoted by $\mathcal{Q} = \{\mathcal{G}_1, \mathcal{G}_2, \mathcal{G}_3...\mathcal{G}_n\}$ representing all possible topologies. Additionally, let $M = \{1, 2, 3..., m\}$ denote the set of indices corresponding to these topologies. The switching communication topology is characterized by a switching graph $G_{\delta(t)}$ where $\delta(t) : [0, +\infty) \to M$ denotes the constant switching signal.

Accordingly, $A_{\delta(t)}$ and $D_{\delta(t)}$ represent, respectively, the switching adjacency matrix and degree matrix of $G_{\delta(t)}$ at time t. We can also get the switching Laplacian matrix

$$L_{\delta(t)} = D_{\delta(t)} - A_{\delta(t)}. \tag{6}$$

C. Consensus Algorithm

Suppose a homogeneous multi-agent system comprising N agents, each of which can be described by the following dynamic equation:

$$\dot{x_i}(t) = \mu_i(t) \quad i \in V(G) = \{1, 2, 3...n\} \tag{7}$$

Here, $x_i(t)$ is a state vector and $\mu_i(t)$ is the control input of the node i. $V(G)$ denotes the set of all nodes on Graph G.

Definition 1 *([12]) The nodes of a multi-agent system have reached a consensus if and only if the states of agents satisfy*

$$\lim_{t\to\infty} |x_i(t) - x_j(t)| = 0 \tag{8}$$

for all $i, j \in V(G)$. Obviously, when the system has reached a consensus, $\boldsymbol{x} \in \mathbb{I}^n = \{\ y \in \mathbb{R}^n | y = c \cdot (1, 1, 1....1)\}$.

Remark 1 *Unlike traditional consensus control scheme which is shown in* (7)*, we indirectly control the system state vector $\boldsymbol{x}(t)$ by controlling the error function $\boldsymbol{e}(t)$ in our novel DFTZNN scheme, which can be summarized as follows:*

$$\dot{\boldsymbol{e}}(t) = \boldsymbol{u}(t) \tag{9}$$

Here, the corresponding control input $\boldsymbol{u}(t)$ is $-\Phi(\boldsymbol{e}(t))$, which is shown in (12)*. In the next section, we will describe the elegant DFTZNN scheme in detail.*

III. The Practical Approach

A. The Distributed Fixed-time Zeroing Neural Network

ZNN encompasses a class of Hopfield-like networks. We can follow three steps to design a specific ZNN model for a given problem. To begin with, we need to define a vector-valued error function, and when the error function converges to zero, the problem is considered solved. Next, we need to select a suitable ZNN design formula from a range of ZNN design formulas, each offering various advanced features. Finally, we can obtain a customized ZNN dynamic equation tailored to address the specific problem at hand.

Supposing a multi-agent system composed of n agents with a switching topology $G_{\delta(t)}$, let's consider the error between node i and its neighboring nodes. This is defined as follows:

$$e_i(t) = \sum_{j=1}^{n} a_{ij}(t)(x_i(t) - x_j(t)), \tag{10}$$

where $a_{ij}(t)$ denotes the element of the switching adjacency matrix $A_{\delta(t)} = [a_{ij}(t)]$.

For the convenience of subsequent discussion, the error can be expressed in vector form:

$$\boldsymbol{e}(t) = L_{\delta(t)}\boldsymbol{x}(t), \tag{11}$$

where $L_{\delta(t)}$ is the switching matrix.

A distributed ZNN scheme [30] is usually in the following form

$$\dot{\boldsymbol{e}}(t) = -\Phi(\boldsymbol{e}(t)), \tag{12}$$

where $\boldsymbol{e}(t)$ is the error function, and $\Phi(x)$ is some certain activation functions.

In order to reach consensus, we construct the following distributed ZNN scheme in the form of the implicit dynamic system:

$$L_{\delta(t)}\dot{\boldsymbol{x}}(t) = -\Phi(L_{\delta(t)}\boldsymbol{x}(t)), \tag{13}$$

where $\Phi(\boldsymbol{x})$ is the Sinh-power activation function (SHAF), and the element-form of $\Phi(\boldsymbol{x})$ is:

$$\phi(x) = h\sinh(|x|^p)\mathrm{sign}(x), \tag{14}$$

where $h > 0$ and $0 < p < 1$ are real parameters. For the convenience of subsequent discussion, we call the novel consensus control scheme (13) the distributed fixed-time zeroing neural network (DFTZNN) scheme.

For the purpose of comparison, let us consider a multi-agent system consisting of n agents with a fixed topology G. To facilitate subsequent discussions, we construct the following implicit dynamic system based on the distributed Zeroing Neural Network (ZNN) method [30]:

$$L\dot{\boldsymbol{x}}(t) = -\Phi(L\boldsymbol{x}(t)), \tag{15}$$

which is a simplified case of (13).

B. Fixed-time Convergence

Generally, a dynamics system can be represented as follows:

$$\dot{\boldsymbol{x}}(t) = f(\boldsymbol{x}(t), t), \tag{16}$$

where $\boldsymbol{x}(t) \in \mathbb{R}^n$ represents the state of the system with $t \in [0, +\infty]$ as a real time variable, and $f(\cdot)$ is a suitable mapping. Assuming the equilibrium point of the system is at the origin, denoted a $\boldsymbol{x}(t) = \mathbf{0}$, we establish the following definitions:

Definition 2 *([30]) We represent the initial state by x_0 , where x_0 denotes the initial condition of the system. In addition, we denote by $\mathcal{T}(\boldsymbol{x_0}) : \mathbb{R}^n \to \mathbb{R}_+ \cup 0$ the settling-time function (STF) where $\|\boldsymbol{e}(t)\|_{t\geqslant\mathcal{T}(\boldsymbol{e}_0)} \equiv 0$, and $\|\boldsymbol{e}(t)\|_{t<\mathcal{T}(\boldsymbol{e}_0)} \neq 0$. For dynamics system* (16)*, if $\mathcal{T}(\boldsymbol{e}_0) < M$ where $M > 0$ is a positive real number, then we call it a fixed-time consensus system.*

Definition 3 *([30]) Considering the dynamics system* (15)*, if the activation function $\Phi(x)$ satisfies the following conditions:*

1) *The vector-valued function $\Phi(x)$ can be decoupled as a group of functions*

$$\Phi(\boldsymbol{e}(t)) = [\phi(e_1(t)), \phi(e_2(t))...\phi(e_n(t))]^{\mathrm{T}}. \tag{17}$$

2) *$\phi(x)$ is a monotone increasing odd function.*
3) *$\phi(x)$ is almost continuous.*

Then we call it a valid activation function (VAF). It is obvious that SHAF (14) *is a VAF.*

Lemma 2 *(Polyakov's theorem [18]) For a ZNN model, if a continuous and positive definite function $\mathcal{V}(t) = f(e(t))$ exists, and satisfy the following condition:*

$$\dot{\mathcal{V}}(t) \leq -(m\mathcal{V}^p(t) + n\mathcal{V}^q(t)), \tag{18}$$

then the ZNN model is fixed-time stable, and the STF is bounded by:

$$\mathcal{T}(\boldsymbol{x}_0) \leq \frac{1}{m(1-p)} + \frac{1}{n(q-1)}. \tag{19}$$

Here, $m > 0$, $n > 0$, $0 < p < 1$, and $q > 1$ are real parameters.

IV. Theoretical Analysis

A. Stability Analysis

In this section, we presented detailed theoretical analysis to prove that the DFTZNN scheme is asymptotically stable, and the consensus is achievable.

Theorem 1 *Considering the DFTZNN model with a switching topology $G_{\delta(t)}$ formed by strongly connected graphs, the dynamic system is asymptotically stable and tend to be consensus.*

Proof *We first transform the DFTZNN design formula into $\dot{\boldsymbol{e}}(t) = -\Phi(\boldsymbol{e}(t))$. Consider each subsystem $\dot{e}_i(t) = -\phi(e_i(t)), i = 1, 2, 3..., n$ and then construct Lyapunov function candidates $v_i(t) = \frac{e_i^2(t)}{2}$ for every component of $\boldsymbol{e}(t)$. By taking the derivative of Lyapunov function candidates $v_i(t)$, we have:*

$$\begin{aligned} \dot{v}_i(t) &= \dot{e}_i(t)e_i(t) \\ &= -\phi(e_i(t))e_i(t). \end{aligned} \tag{20}$$

Since SHAF (14) *is a VAF, it is obvious that $x \cdot \phi(x) > 0$ and $\phi(x) = 0$ if and only if $x = 0$, we have*

$$\phi(e_i(t))e_i(t) = \begin{cases} > 0, & \text{if } e_i(t) \neq 0. \\ = 0, & \text{if } e_i(t) = 0, \end{cases} \tag{21}$$

Obviously $\dot{v}_i(t) \leq 0$, so the dynamic system is asymptotically stable. The consensus is obtained from $\lim_{t\to\infty} e_i(t) = 0, i = 1, 2, 3..., n$ and Lemma 1.

B. Fixed-time Convergence

As a general framework, we are able to use many established results of ZNN in existing literature [21]–[23]. In this section, to illustrate the superiority of ZNN, we will prove that the proposed DFTZNN scheme is fixed-time stable, and then estimate the upper bound of the STF through both the traditional Polyakov's theorem and the novel integral-based method from previous studies on ZNN [30].

Remark 2 *Considering the DFTZNN scheme* (13) *established under a switching topology, it reduces to* (15) *if the multi-agent system only has one topology structure. In the subsequent discussion, we will see that DFTZNN scheme* (13) *is fixed-time stable, and the upper bounds of the settling-time functions are independent of initial states and topology structures. Hence, the following theory is analyzed based on* (15) *under a fixed topology for convenience.*

Theorem 2 *Considering the DFTZNN scheme, according to Lemma 2, we can prove that it is fixed-time stable and the settling-time function is bounded by:*

$$\mathcal{T}(\boldsymbol{x}_0) \leq \frac{1}{h}\left(\frac{1}{1-p} + \frac{(2k-1)!}{[(2k-1)p-1]}\right), \tag{22}$$

where $\boldsymbol{x}_0$ is the initial state, $h > 0$ and $0 < p < 1$ are parameters defined in (14)*, $k > 0$ is a real constant satisfying $(2k-1)p > 1$ and $(2k-3)p < 1$.*

Proof *We first transform the DFTZNN design formula into $\dot{\boldsymbol{e}}(t) = -\Phi(\boldsymbol{e}(t))$ for the convenience of subsequent discussion, and then construct positive definite auxiliary functions $v_i(t) = |e_i(t)|$ for every component of $\boldsymbol{e}(t)$. By taking the derivative of auxiliary functions $v_i(t)$, we have:*

$$\begin{aligned} \dot{v}_i(t) &= |\dot{e}_i(t)| \\ &= -\phi(e_i(t))\text{sign}(e_i(t)) \\ &= -h\sinh(|e_i(t)|^p) \\ &= -h(|e_i(t)|^p + \frac{|e_i(t)|^{3p}}{6} + \sum_{m=3}^{\infty}\frac{|e_i(t)|^{(2m-1)p}}{(2m-1)!}), \end{aligned} \tag{23}$$

where $h > 0$ and $0 < p < 1$ are parameters defined in (14)*.*

We can always find $k \in \mathbb{N}$ satisfying $(2k-1)p > 1$ and $(2k-3)p < 1$, then:

$$\begin{aligned} \dot{v}_i(t) &= -h(|e_i(t)|^p + \frac{|e_i(t)|^{3p}}{6} + \sum_{m=3}^{\infty}\frac{|e_i(t)|^{(2m-1)p}}{(2m-1)!}) \\ &\leq -h(|e_i(t)|^p + \frac{|e_i(t)|^{(2k-1)p}}{(2k-1)!}) \end{aligned} \tag{24}$$

According to Lemma 2, we can estimate the upper bound of the settling-time function for every component of $\boldsymbol{e}(t)$:

$$T_i(\boldsymbol{x}_0) \leq \frac{1}{h}\left(\frac{1}{1-p} + \frac{(2k-1)!}{[(2k-1)p-1]}\right). \tag{25}$$

Further, we can conclude that:

$$\mathcal{T}(\boldsymbol{x}_0) = \max_{i\in\mathbb{N}_+} T_i(\boldsymbol{x}_0) \leq \frac{1}{h}\left(\frac{1}{1-p} + \frac{(2k-1)!}{[(2k-1)p-1]}\right), \tag{26}$$

where $\boldsymbol{x}_0$ is the initial state, $h > 0$ and $0 < p < 1$ are parameters defined in (14)*, $\Gamma(s) = \int_0^\infty t^{s-1}\exp(-t)\mathrm{d}t$ is the Euler Γ function, and $\zeta(s) = \sum_{k=1}^{\infty} k^{-s}$ is the Riemann ζ function.*

Theorem 3 *Considering the DFTZNN scheme, by the novel integral-based method proposed in previous studies on ZNN [30], we can prove that it is fixed-time stable and the settling-time function is bounded by:*

$$\mathcal{T}(\boldsymbol{x}_0) = \frac{2 - 2^{1-1/p}}{hp}\Gamma\left(1 + 1/p\right)\zeta\left((1/p)\right), \tag{27}$$

where $\boldsymbol{x}_0$ is the initial state, $h > 0$ and $0 < p < 1$ are parameters defined in (14)*, $\Gamma(s) = \int_0^\infty t^{s-1}\exp(-t)\mathrm{d}t$ is the Euler Γ function, $\zeta(s) = \sum_{k=1}^{\infty} k^{-s}$ is the Riemann ζ function.*

Proof *Firstly, we introduce the novel integral-based method [30] briefly. We denote $e_0^{max} = \max\{|e_0^1|, |e_0^2|, ..., |e_0^n|\}$ the absolute least upper bound of the initial error. Then, we*

can estimate the upper bound of the settling-time function as follows:

$$\begin{aligned}\mathcal{T}(\boldsymbol{x}_0) &= \sup_{i\in\mathbb{N}_+}\{\mathcal{T}(e_0^i)\}\\ &= \int_0^{e_0^{max}} \frac{1}{\phi(e)}\mathrm{d}e\end{aligned} \tag{28}$$

For the convenience of subsequent discussion, we transform the DFTZNN design formula into $\dot{\boldsymbol{e}}(t) = -\Phi(\boldsymbol{e}(t))$*. According to Definition 2, we consider the extreme situation, i.e.* $e_0^{max} \to \infty$*, we have:*

$$\begin{aligned}\mathcal{T}(\boldsymbol{e}_0) &= \int_0^{\infty} \frac{1}{\phi(e)}\mathrm{d}e\\ &= \int_0^{\infty} \frac{1}{h\sinh(e^p)}\mathrm{d}e\\ &= \int_0^{\infty} \frac{y^{1/p-1}}{hp\sinh(y)}\mathrm{d}y\\ &= \frac{2-2^{1-1/p}}{hp}\Gamma\left(1+1/p\right)\zeta\left((1/p)\right),\end{aligned} \tag{29}$$

where $h > 0$ *and* $0 < p < 1$ *are parameters defined in* (14)*,* $\Gamma(s) = \int_0^{\infty} t^{s-1}\exp(-t)\mathrm{d}t$ *is the Euler* Γ *function, and* $\zeta(s) = \sum_{k=1}^{\infty} k^{-s}$ *is the Riemann* ζ *function.*

C. Robust Analysis

In this section, we provide a thorough theoretical analysis to demonstrate that the DFTZNN scheme is robust in the presence of the bounded noise. Based on (15), we denote $\boldsymbol{w}(t)$ as the bounded noise which satisfying $\|\boldsymbol{w}(t)\|_2 < m$, and then the following perturbed DFTZNN scheme can be derived:

$$L\dot{\boldsymbol{x}}(t) = -\Phi(L\boldsymbol{x}(t)) + \boldsymbol{w}(t), \tag{30}$$

Theorem 4 *Considering the DFTZNN scheme, it is robust under the bounded noise* $\boldsymbol{w}(t)$*. If* $\|\boldsymbol{w}(t)\|_2 < m$*, then the error* $\|\boldsymbol{e}(t)\|_2$ *over time is bounded by*

$$\|\boldsymbol{e}(t)\|_2 \le \frac{m}{2\upsilon}\sqrt{n}(1+\sqrt{n}). \tag{31}$$

Here, υ *is a constant satisfying* $\upsilon \ge 1$*.*

Proof: Firstly, take the derivative of $\mathcal{F}(t) = \frac{1}{2}\|\boldsymbol{e}(t)\|_2^2$ to obtain

$$\begin{aligned}\dot{\mathcal{F}}(t) &= \boldsymbol{e}^{\mathrm{T}}(t)\dot{\boldsymbol{e}}(t)\\ &= -\boldsymbol{e}^{\mathrm{T}}(t)(\Phi(\boldsymbol{e}(t)) - \boldsymbol{w}(t))\\ &< -\sum_{i=1}^{n}|e_i(t)|(\phi(|e_i(t)|) - m).\end{aligned} \tag{32}$$

Here, $\mathcal{F}(t)$ is a Lyapunov function candidate which is used to determine whether the multi-agent system is stable or not in this study.

To further discuss the stability, we will need a auxiliary function $g(e_k(t)) = \phi(e_k(t)) - m$, and the following inequities can be derived:

$$\begin{cases}\dot{\mathcal{F}}(t) \le 0 & \text{if } \forall k, g(e_k(t)) \ge 0,\\ \dot{\mathcal{F}}(t) \le m & \text{if } \exists k, g(e_k(t)) < 0,\end{cases} \tag{33}$$

where $m > 0$ is a constant.

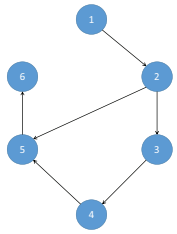

Fig. 1: The communication topology $\mathcal{G}_1$ of a multi-agent system composed of $n = 6$ agents.

In the case where $\dot{\mathcal{F}}(t) \le 0$, the stability of the multi-agent system can be obtained easily through the Lypuyanov stability theorem and no further discussion is needed. Therefore, we should put more emphasis on the case $0 \le \dot{\mathcal{F}}(t) \le m$ which is analyzed thoroughly in the subsequent discussion.

In the case where $0 \le \dot{\mathcal{F}}(t) \le m$, make $\upsilon = \phi(|e_i(t)|)/|e_i(t)| \geqslant 1$ and $\omega = \frac{m}{\upsilon}$ to obtain:

$$\dot{\mathcal{F}}(t) \leqslant -\upsilon\sum_{i=1}^{n}|e_i(t)|(|e_i(t)| - \omega). \tag{34}$$

It is obvious that $\|\boldsymbol{e}(t)\|_2$ and $\mathcal{F}(t)$ are increasing as $0 \le \dot{\mathcal{F}}(t) \le m$. When $\dot{\mathcal{F}}(t) = 0$, we have $\sum_{i=1}^{n^2}|e_i(t)|(|e_i(t)| - w) = 0$ and $\|\boldsymbol{e}(t)\|_2$ achieves the maximum.

Let $h(x) = x(x-w)$, and $|e_l(t)|$ denotes as the maximum term of $|e_j(t)|$. We know $h_{\min}(x) = h(\frac{w}{2}) = -\frac{w^2}{4}$. Then we have:

$$\begin{aligned}|e_l(t)|(|e_l(t)| - w) &= -\sum_{i=1,i\neq l}^{n}|e_i(t)|(|e_i(t)| - w)\\ &\le (n-1)\frac{w^2}{4}.\end{aligned} \tag{35}$$

From (35), $|e_l(t)| \le \frac{(1+\sqrt{n})w}{2}$ can be derived to obtain

$$\begin{aligned}\|\boldsymbol{e}(t)\|_2 &\leqslant \sqrt{\sum_{i=1}^{n}(|e_l(t)|)^2}\\ &\leqslant \sqrt{n\Big[\frac{(1+\sqrt{n})w}{2}\Big]^2}\\ &= \frac{w}{2}\sqrt{n}(1+\sqrt{n})\\ &= \frac{m}{2\upsilon}\sqrt{n}(1+\sqrt{n}).\end{aligned} \tag{36}$$

V. Numerical Verification

In the subsequent discussion, the DFTZNN scheme will be used in our experiments, and the common parameters are set to $h = 1$ and $p = 0.5$.

According to Theorem 2, we can conclude that $k = 2$, and then the settling time function is bounded by:

$$\begin{aligned}\mathcal{T}(\boldsymbol{x}_0) &\le \frac{1}{h}\left(\frac{1}{1-p} + \frac{(2k-1)!}{[(2k-1)p-1]}\right)\\ &= \frac{1}{1-0.5} + \frac{3!}{[3\times 0.5 - 1]}\\ &= 14\end{aligned} \tag{37}$$

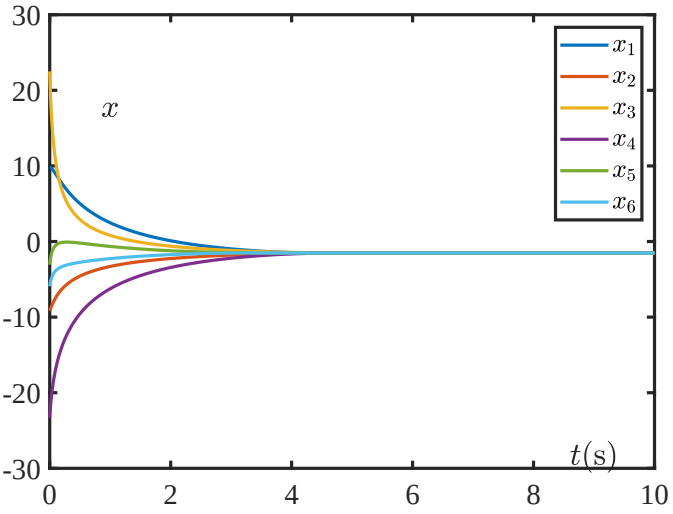

Fig. 2: The state of the multi-agent system in Example 1 under a fixed topology

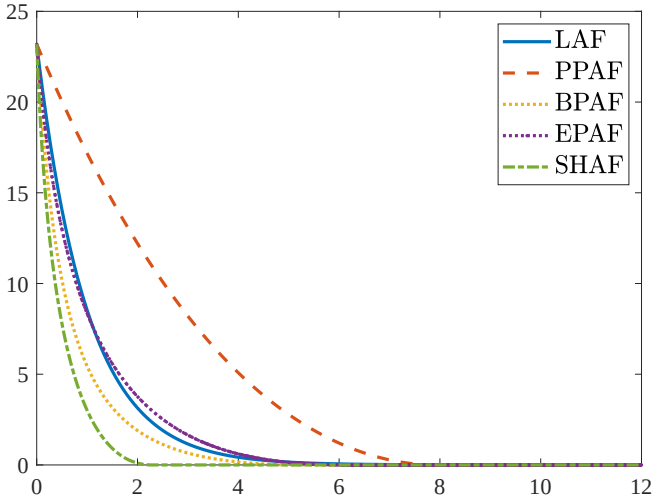

Fig. 3: Error of the DFTZNN scheme for Example 2 using five activation functions.

According to Theorem 3, the settling time function is bounded by:

$$\begin{aligned}\mathcal{T}(\boldsymbol{e}_0) &= \frac{2-2^{1-1/p}}{hp}\Gamma\left(1+1/p\right)\zeta\left((1/p)\right) \\ &= \frac{\pi^2}{2} \approx 4.93\end{aligned} \tag{38}$$

A. Fixed-Time Consensus Under Fixed Topology

Example 1 *In this example, the multi-agent system is composed of $n = 6$ agents, and we present its communication topology $\mathcal{G}_1$ in Fig. 1. $\mathcal{G}_1$ is represented as a strongly connected graph, and the cardinality of its edge set is $|\mathcal{E}(\mathcal{G}_1)| = 6$. The DFTZNN scheme is used in our experiment.*

In this experiment, we set the initial condition $\boldsymbol{x}_0 = [9.7414, -9.1450, 22.5111, -23.2776, -3.0627, -5.9220]$. *Under the control of DFTZNN scheme, the state of six*

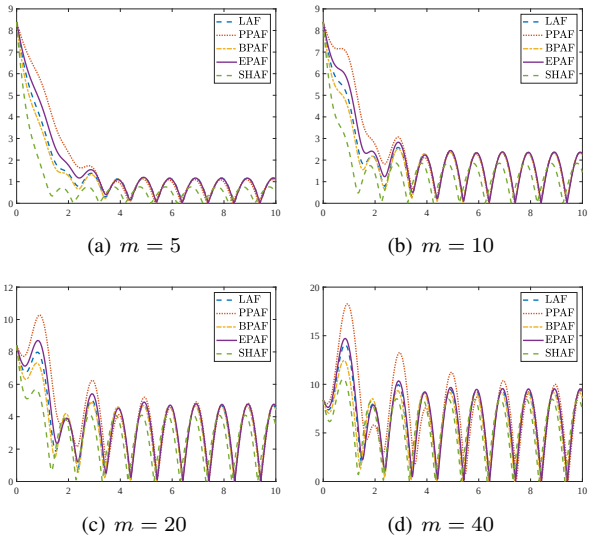

(a) $m = 5$ (b) $m = 10$

(c) $m = 20$ (d) $m = 40$

Fig. 4: The trajectories of error over time under the control of DFTZNN scheme with different m.

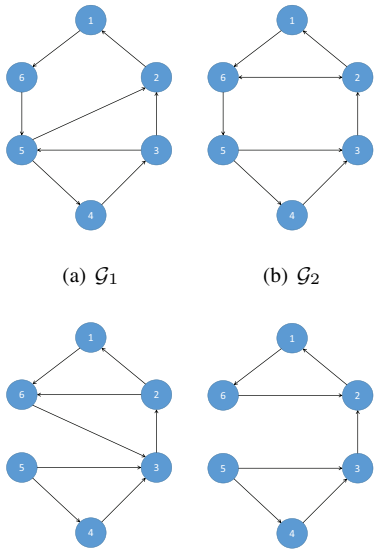

(a) $\mathcal{G}_1$ (b) $\mathcal{G}_2$

(c) $\mathcal{G}_3$ (d) $\mathcal{G}_4$

Fig. 5: The set of switching topologies in Examples 4, 5 and 6.

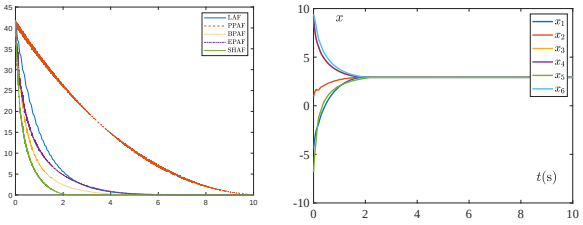

(a) The trajectories of error (b) The trajectories of state

Fig. 6: The multi-agent system with two switching topologies reaches consensus under the control of DFTZNN scheme.

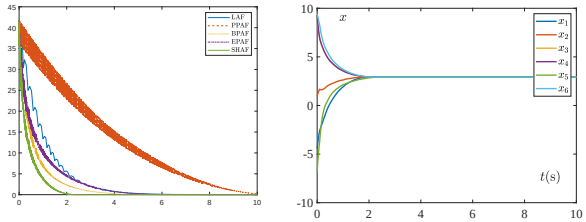

(a) The trajectories of error (b) The trajectories of state

Fig. 7: The multi-agent system with three switching topologies reaches consensus under the control of DFTZNN scheme.

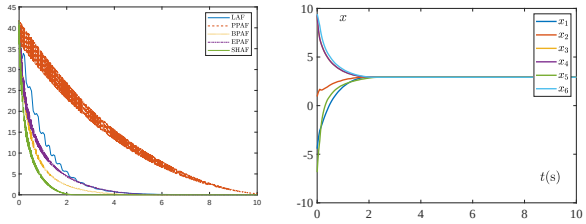

(a) The trajectories of error (b) The trajectories of state

Fig. 8: The multi-agent system with four switching topologies reaches consensus under the control of DFTZNN scheme.

agents is shown in Fig. 2, and the system converged within approximately 5 *seconds, which verified our theoretical analysis further. In comparison with the traditional Polyakov's theorem [18], our novel method for estimating the upper bound proves to be more accurate.*

Example 2 *Considering the same multi-agent system shown in Example 1, in addition to the DFTZNN scheme activated by SHAF* (14)*, we will present other four widely used activation functions for comparison purpose, i.e.,*

1) *Linear activation function (LAF):* $\psi(e) = e$*;*
2) *P-power activation function (PAF):* $\psi(e) = |e|^{0.5}\text{sign}(e)$*;*
3) *Bi-power activation function (BPAF):* $\psi(e) = \frac{1}{2}(|e|^{0.5} + |e|^{1.5})\text{sign}(e)$*;*
4) *Exp-power activation function (EPAF):* $\psi(e) = \frac{1}{2}(\exp(|e|^{0.5}) - 1) \cdot \text{sign}(e)$*;*

In this experiment, we initialize the system with the initial condition $\boldsymbol{x}_0 = [3.7842, 4.9630, -0.9891, -8.3235, -5.4204, 8.2667]$*. Since the original error function is a vector function, which may not be convenient for demonstration, we utilize the 2-norm of the error as the performance measure. Subsequently, under the control of the Distributed Fixed-Time Zeroing Neural Network (DFTZNN) scheme employing five activation functions, the error is depicted in Fig. 3.*

Looking at Fig. 3, the DFTZNN scheme activated by the novel SHAF (14) *proposed in our study has better convergence than the classic linear scheme and the scheme activated by other activation functions.*

Example 3 *In the context of the same multi-agent system as presented in Example 1, we extend our investigation. In addition to the DFTZNN scheme activated by SHAF* (14)*, we incorporate four other widely used activation functions,*

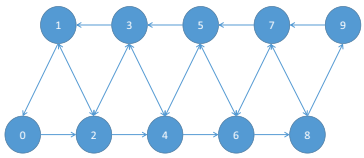

Fig. 9: The communication topology $\mathcal{G}_2$ of the UAV formation.

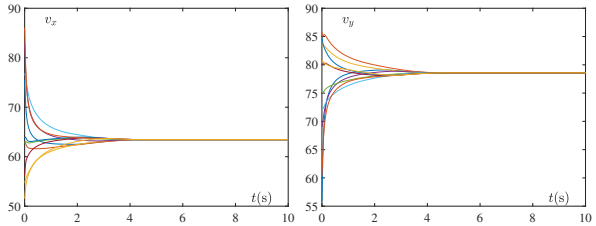

(a) The X-axis component (b) The Y-axis component

Fig. 10: The velocity component of the formation under th31.2e control of the SBP-DFTZNN scheme.

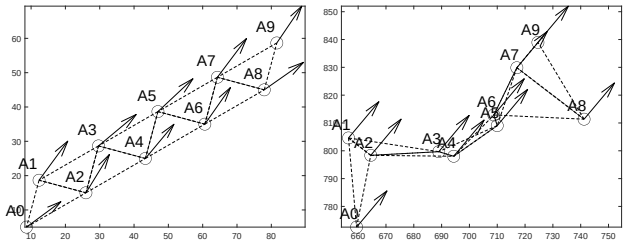

(a) The initial state (b) The final state

Fig. 11: The initial state and the final state of the formation after 10 seconds, where the arrow represents the velocity vector.

namely, LAF, PAF, BPAF, and EPAF, as outlined in Example 2, for the purpose of comparison. Common parameters are set consistently with those in Example 2.

In this experiment, we initialize the system with the initial condition $\boldsymbol{x}_0 = [1.7873, 2.5774, 2.4313, -1.0777, 1.5547, -3.2881]$*. Since the original error function is a vector function, which may not be convenient for demonstration, we utilize the 2-norm of the error as the performance measure. The following bounded noise are added to the experiment to verify the robustness of the proposed DFTZNN scheme:*

$$w_i(t) = m\sin(10t) \quad i \in \{1, 2, 3, ..., n\}, \tag{39}$$

where $w_i(t)$ *is the* i*th element of the bounded noise satisfying* $|w_i(t)| < m$*.*

Four different sets of parallel experiments are designed to verify the robustness of the DFTZNN scheme, and in each set of experiments, the upper bounds are respectively $5, 10, 20, 40$*. Then, under the control of the DFTZNN scheme using five activation functions, the error is shown in Fig. 4. Looking at Fig. 4, the DFTZNN scheme activated by five different activation functions is robust under bounded noise.*

TABLE I: Initial position and velocity of the formation.

#	Position	Velocity
0	(75.5341,55.8527)	(8.6603,5.0000)
1	(62.9923,85.7919)	(12.3205,18.6603)
2	(51.5482,84.0502)	(25.9808,15.0000)
3	(82.7542,69.0142)	(29.6410,28.6603)
4	(62.6993,75.0884)	(43.3013,25.0000)
5	(76.8715,72.0846)	(46.9615,38.6603)
6	(56.1667,80.2293)	(60.6218,35.0000)
7	(63.7977,84.8645)	(64.2820,48.6603)
8	(86.0756,60.3102)	(77.9423,45.0000)
9	(54.7464,80.7368)	(81.6025,58.6603)

B. Fixed-Time Consensus Under Switching Topology

Example 4 *Taking into account a multi-agent system with a switching topology comprising $n = 6$ agents, where all possible topologies are represented by a set of strongly connected graphs $\mathcal{Q} = \{\mathcal{G}_1, \mathcal{G}_2\}$ shown in Fig. 5. The DFTZNN scheme activated by five aforementioned activation functions (i.e., SHAF, LAF, PAF, BPAF and EPAF) will be used in our experiment. We set the initial condition $\boldsymbol{x}_0 = [-1.6546, -9.0069, 8.0543, 8.8957, -0.1827, -0.2149]$. Then, under the control of the DFTZNN scheme, the trajectories of error over time are shown in Fig. 6(a). Specifically, the state of the agents under the control of the DFTZNN scheme activated by SHAF* (14) *is shown in Fig. 6(b).*

As shown in Fig. 6, the multi-agent system with two switching topologies reached consensus under the control of the DFTZNN scheme activated by five aforementioned functions. Specifically, when controlled by the DFTZNN scheme activated by SHAF eqrefshaf, the multi-agent system reached consensus after approximately 5 seconds, which is consistent with our theoretical analysis that it converges in approximately 4.93 seconds.

Example 5 *Considering a similar multi-agent in Example 4, the set of all possible topologies is represented by $\mathcal{Q} = \{\mathcal{G}_1, \mathcal{G}_2, \mathcal{G}_3\}$, and is shown in Fig. 5. The DFTZNN scheme activated by five aforementioned activation functions (i.e., SHAF, LAF, PAF, BPAF and EPAF) will be used in our experiment. We set the same initial condition as Example 4. Then, under the control of the DFTZNN scheme, the trajectories of error over time are shown in Fig. 7(a). Specifically, the state of the agents under the control of the DFTZNN scheme activated by SHAF* (14) *is shown in Fig. 7(b).*

As shown in Fig. 7, the multi-agent system with two switching topologies reached consensus under the control of the DFTZNN scheme activated by five aforementioned functions. Specifically, when controlled by the DFTZNN scheme activated by SHAF (14)*, the multi-agent system reached consensus after approximately 5 seconds, which is consistent with our theoretical analysis that it converges in approximately 4.93 seconds.*

Example 6 *Considering a similar multi-agent in Example 4, the set of all possible topologies is represented by $\mathcal{Q} = \{\mathcal{G}_1, \mathcal{G}_2, \mathcal{G}_3, \mathcal{G}_4\}$ which is shown in Fig. 5. The DFTZNN scheme activated by five aforementioned activation functions (i.e., SHAF, LAF, PAF, BPAF and EPAF) will be used in our experiment. Set the same initial condition as Example 4. Then, under the control of the DFTZNN scheme, the trajectories of error over time are shown in Fig. 8(a). Specifically, the state of the agents under the control of the DFTZNN scheme activated by SHAF* (14) *is shown in Fig. 8(b).*

As shown in Fig. 8, the multi-agent system with two switching topologies reached consensus under the control of the DFTZNN scheme activated by five aforementioned functions. Specifically, when controlled by the DFTZNN scheme activated by SHAF (14)*, the multi-agent system reached consensus after approximately 5 seconds, which is consistent with our theoretical analysis that it converges in approximately 4.93 seconds.*

C. A Practical Application

Formation control represents a typical consensus problem in multi-agent systems, where several robots collaborate to form a specific arrangement. Each robot adjusts its behavior to align with neighboring robots, ensuring consistent speed and heading. In this section, we leverage the distributed fixed-time zeroing neural network (DFTZNN) scheme to synchronize all robots in the system, maintaining uniform speed and direction.

For the sake of visualization convenience, this paper focuses on the two-dimensional plane. However, it's worth noting that the proposed protocol can be readily extended to a three-dimensional case.

Example 7 *Considering a formation composed of 10 robots which communication topology is shown in Fig. 9, the initial velocity and position are shown in Table I and Fig. 11(a). In this experiment, the velocity is regarded as a two-dimensional vector $(\boldsymbol{v_x}, \boldsymbol{v_y})$, and the velocity consensus obviously includes the direction consensus. Therefore, we only need to control the state of velocity. The velocity of the formation under the control of the DFTZNN scheme activated by SHAF* (14) *is shown in Fig. 10. It should converge in 4.93 seconds according to Theorem 2, and numerical experiment results verify our theoretical results. The final state of the formation after 10 seconds is shown in Fig. 11(b).*

VI. Conclusion

ZNN, recognized as a systematic approach, proves to be a potent tool for designing effective control schemes. Despite its potential, there has been limited exploration of ZNN's application in multi-agent systems. In this study, leveraging ZNN, we introduce the DFTZNN control scheme to achieve fixed-time and robust consensus among multi-agents. This novel approach offers researchers a novel perspective for investigating consensus problems. We highlight the superiority of this ZNN-based methods by exemplifying the upper bound estimation of the settling-time function. Comprehensive theoretical analysis and numerical experiments further validate the effectiveness of the proposed method.

However, it is essential to acknowledge certain limitations of ZNN-based methods. These approaches are not as intuitive as

traditional consensus control schemes, requiring the definition of an error function as a preliminary step. Additionally, ZNN-based methods may not be suitable for achieving average consensus, which is another import topic in consensus research.

REFERENCES

[1] M. Minsky, "The society of mind," in *The Personalist Forum*, vol. 3, no. 1. JSTOR, 1987, pp. 19–32.

[2] J. A. V. Trejo, D. Rotondo, M. A. Medina, and D. Theilliol, "Robust observer-based leader-following consensus for a class of nonlinear multi-agent systems: application to UAV formation control," in *IEEE Int. Conf. on UAV (ICUAS)*. Athens, Greece, 2021, pp. 1565–1572.

[3] M. Bozuyla and A. T. Tola, "Designing a novel transportation system using microscopic models and multi-agent approach," *Autom. Control Comput. Sci.*, vol. 55, no. 2, pp. 125–136, 2021.

[4] L. Xiang, Y. Tan, G. Shen, and X. Jin, "Applications of multi-agent systems from the perspective of construction management: A literature review," *Eng. Constr. Archit. Manag.*, 2021.

[5] M. Panda and B. Das, "Multi-agent system of autonomous underwater vehicles in octagon formation," in *Intel Syst.* Springer, 2021, pp. 125–138.

[6] M. Azeroual, T. Lamhamdi, H. El Moussaoui, and H. El Markhi, "Simulation tools for a smart grid and energy management for microgrid with wind power using multi-agent system," *Wind Eng.*, vol. 44, no. 6, pp. 661–672, 2020.

[7] J. Yu, S. Yu, J. Li, and Y. Yan, "Fixed-time consensus of multi-agent system under time varying topology," in *IECON 2017-43rd Annu. Conf. IEEE Ind. Electron. Soc.* IEEE, 2017, pp. 5546–5551.

[8] J. Yu, S. Yu, and Y. Yan, "Fixed-time stability of stochastic nonlinear systems and its application into stochastic multi-agent systems," *IET Control Theory Appl.*, vol. 15, no. 1, pp. 126–135, 2021.

[9] J. Yu, S. Yu, J. Li, and Y. Yan, "Fixed-time stability theorem of stochastic nonlinear systems," *Int. J. Control*, vol. 92, no. 9, pp. 2194–2200, 2019.

[10] W. Zhao, H. Chu, M. Zhang, T. Sun, and L. Guo, "Flocking control of fixed-wing uavs with cooperative obstacle avoidance capability," *IEEE Access*, vol. 7, pp. 17 798–17 808, 2019.

[11] T. Wang and J. Huang, "Leader-following adaptive consensus of multiple uncertain rigid body systems over jointly connected networks," *Unmanned Syst.*, vol. 8, no. 02, pp. 85–93, 2020.

[12] R. Olfati-Saber and R. M. Murray, "Consensus problems in networks of agents with switching topology and time-delays," *IEEE Trans. Autom. Control*, vol. 49, no. 9, pp. 1520–1533, 2004.

[13] G. Dong, H. Li, H. Ma, and R. Lu, "Finite-time consensus tracking neural network FTC of multi-agent systems," *IEEE Trans. Neural Netw. Learning Syst.*, vol. 32, no. 2, pp. 653–662, 2020.

[14] Y. Li, C. Wang, X. Cai, L. Li, and G. Wang, "Neural-network-based distributed adaptive asymptotically consensus tracking control for nonlinear multiagent systems with input quantization and actuator faults," *Neurocomputing*, vol. 349, pp. 64–76, 2019.

[15] J. Liu, Y. Zhang, Y. Yu, and C. Sun, "Fixed-time leader–follower consensus of networked nonlinear systems via event/self-triggered control," *IEEE Trans. Neural Netw. Learning Syst.*, vol. 31, no. 11, pp. 5029–5037, 2020.

[16] X. Liu, J. Cao, and C. Xie, "Finite-time and fixed-time bipartite consensus of multi-agent systems under a unified discontinuous control protocol," *J. Frankl. Inst.-Eng. Appl. Math.*, vol. 356, no. 2, pp. 734–751, 2019.

[17] Y. Guo, Y. Tian, Y. Ji, and Z. Ge, "Fixed-time consensus of nonlinear multi-agent system with uncertain disturbances based on event-triggered strategy," *ISA Trans.*, vol. 126, pp. 629–637, 2022.

[18] A. Polyakov, "Nonlinear feedback design for fixed-time stabilization of linear control systems," *IEEE Transactions on Automatic Control*, vol. 57, no. 8, pp. 2106–2110, 2012.

[19] M. Yang, Y. Zhang, N. Tan, and H. Hu, "Concise discrete znn controllers for end-effector tracking and obstacle avoidance of redundant manipulators," *IEEE Transactions on Industrial Informatics*, vol. 18, no. 5, pp. 3193–3202, 2021.

[20] D. Chen, S. Li, Q. Wu, and X. Luo, "Super-twisting znn for coordinated motion control of multiple robot manipulators with external disturbances suppression," *Neurocomputing*, vol. 371, pp. 78–90, 2020.

[21] L. Xiao, L. Jia, Y. Wang, J. Dai, Q. Liao, and Q. Zhu, "Performance analysis and applications of finite-time znn models with constant/fuzzy parameters for tvqpei," *IEEE Trans. Neural Netw. Learning Syst.*, pp. 1–12, 2021.

[22] J. Dai, Y. Li, L. Xiao, L. Jia, Q. Liao, and J. Li, "Comprehensive study on complex-valued ZNN models activated by novel nonlinear functions for dynamic complex linear equations," *Inform. Sci.*, vol. 561, pp. 101–114, 2021.

[23] L. Xiao, Y. Zhang, J. Dai, K. Chen, S. Yang, W. Li, B. Liao, L. Ding, and J. Li, "A new noise-tolerant and predefined-time ZNN model for time-dependent matrix inversion," *Neural Netw.*, vol. 117, pp. 124–134, 2019.

[24] C. Deng, W. Che, and Z. Wu, "A dynamic periodic event-triggered approach to consensus of heterogeneous linear multiagent systems with time-varying communication delays," *IEEE Trans. Cybern.*, vol. 51, no. 4, pp. 1812–1821, 2020.

[25] X. Jiang, G. Xia, Z. Feng, and Z. Jiang, "Consensus tracking of data-sampled nonlinear multi-agent systems with packet loss and communication delay," *IEEE Trans. Netw. Sci. Eng.*, vol. 8, no. 1, pp. 126–137, 2020.

[26] X. Li, Q. Zhou, P. Li, H. Li, and R. Lu, "Event-triggered consensus control for multi-agent systems against false data-injection attacks," *IEEE Trans. Cybern.*, vol. 50, no. 5, pp. 1856–1866, 2019.

[27] "Consensus switching of second-order multiagent systems with time delay," *IEEE Trans. Cybern.*, vol. 52, no. 5, pp. 3349–3353, 2022.

[28] Z. Liu, G. Wen, X. Yu, Z. Guan, and T. Huang, "Delayed impulsive control for consensus of multiagent systems with switching communication graphs," *IEEE Trans. Cybern.*, vol. 50, no. 7, pp. 3045–3055, 2019.

[29] R. Mu, A. Wei, H. Li, and Z. Wang, "Event-triggered leader-following consensus for multi-agent systems with external disturbances under fixed and switching topologies," *IET Contr. Theory Appl.*, vol. 14, no. 11, pp. 1486–1496, 2020.

[30] L. Xiao, Y. Cao, J. Dai, L. Jia, and H. Tan, "Finite-time and predefined-time convergence design for zeroing neural network: Theorem, method, and verification," *IEEE Trans. Ind. Inform.*, vol. 17, no. 7, pp. 4724–4732, 2020.